

Segmental nitrogen doping and carboxyl functionalization of multi-walled carbon nanotubes

^{Q1} Gergo Peter Szekeres¹, Krisztian Nemeth¹, Aniko Kinka^{1,2}, Melinda Magyar², Balazs Reti¹, Erika Varga³, Zsolt Szegeletes⁴, Andras Erdohelyi³, Laszlo Nagy², and Klara Hernadi^{*,1}

¹ Department of Applied and Environmental Chemistry, University of Szeged, Rerrich Béla tér 1, H-6720 Szeged, Hungary

² Department of Medical Physics and Informatics, University of Szeged, Rerrich Béla tér 1, H-6720 Szeged, Hungary

³ Department of Physical Chemistry and Material Science, University of Szeged, Rerrich Béla tér 1, H-6720 Szeged, Hungary

⁴ Institute of Biophysics, Biological Research Center, Hungarian Academy of Sciences, Temesvári krt. 62, H-6726 Szeged, Hungary

Received 25 March 2015, revised 22 June 2015, accepted 25 June 2015

Published online 00 Month 2015

Keywords carboxyl functionalization, multi-walled carbon nanotubes, protein linking, segmental nitrogen doping

* Corresponding author: e-mail hernadi@chem.u-szeged.hu, Phone: +36 62 544 626, Fax: +36 62 544 626

Partial nitrogen doping was performed during the catalytic chemical vapor deposition (CCVD) synthesis of multi-walled carbon nanotubes. A special reactor was created to facilitate the execution of syntheses with different reaction conditions. The synthesized samples were analyzed by transmission electron microscopy (TEM) in order to provide information about the tubular and nontubular morphology of particles and their deformation gained after the reaction conditions were changed. The incorporation of nitrogen into the carbon structure was studied by X-ray photoelectron spectroscopy (XPS), whereas X-ray diffraction (XRD) and Raman spectroscopy evaluations showed the degree of graphitization. The samples then were carboxyl functionalized in varied concentrations of nitric acid solutions and photosynthetic reaction

center protein (RC-26) purified from purple bacteria was linked to the carboxyl groups in order to make the degree of functionalization visible. The protein-linked samples were characterized by atomic force microscopy (AFM). Our experiments indicated that the syntheses carried out in the new reactor were successful and resulted in carbon nanotubes partially doped with nitrogen. TEM studies revealed that the expected deformations are localized only in a defined segment of carbon nanotubes therefore nitrogen doping is most possibly presented there. The nitrogen content in the samples represented in atomic ratios was between 0.9% and 2.9%. The deformations facilitate the functionalization at that certain area, thus the location of carboxyl groups can be determined.

© 2015 WILEY-VCH Verlag GmbH & Co. KGaA, Weinheim

1 Introduction Carbon nanotubes (CNTs) have been being in the center of scientific interests as the first publication about their existence [1]. Their outstanding electrical [2] and mechanical properties [3] associated with their remarkably low density make them the perfect material for a wide spectrum of industrial utilizations [4, 5]. In a lot of cases, the chemical inertness represented by CNTs is needed for a certain method but otherwise modifications could be required. Two groups of modification techniques should be distinguished: surface modifications, either they are physical or chemical processes, such as surface coating or functionalization, and the modification of the CNT matrix itself by doping it with heteroatoms.

Surface modification techniques are usually applied when CNTs are intended to participate in bio- or physical chemical processes such as drug delivery, targeted accumulation of biological recognition elements (e.g., enzymatic reactions, antiviral, and antibacterial targeting [6]) or strengthening other materials where a perfectly homogeneous medium is essential [7–11]. Doping mechanisms are used when mainly the intrinsic physical properties of the CNTs are required to be modified [12–16]. In most cases, nitrogenous compounds are used as doping precursors because nitrogen incorporation causes different favorable changes in the characteristics of CNTs, such as enhanced conductivity, chemical reactivity, better dispersion in polar media, etc. [17–20]. This most likely

occurs by the one extra 2p electron compared to carbon atoms, provided by the dopant nitrogen atoms [17]. However, the cytotoxicity of nitrogen-doped CNTs is somewhat a lower risk factor than the cytotoxicity of pristine CNTs [21]. Protein linking can be an interesting and efficient route to investigate the effects of CNTs in biomedical systems. This not only facilitates the use of CNTs in varied industrial and scientific fields but also brings it one step closer to in vivo medical applications as well [22–24].

In this study, our aims were to apply different nitrogen doping methods and the development of a new technique for segmental nitrogen doping of multi-walled carbon nanotubes (MWCNTs). Transmission electron microscopy (TEM), X-ray diffractometry (XRD), Raman spectroscopic, and X-ray photoelectron spectroscopic (XPS) data were then evaluated to investigate the results of the experiments. Carboxyl functionalization and then protein linking were used to make the changes visible under an atomic force microscope (AFM).

2 Experimental

2.1 Chemicals

Fe(III)-acetylacetonate (99.9%, Sigma–Aldrich) and Co(II)-acetylacetonate (97%, Sigma–Aldrich) were used as catalysts on CaCO₃ support provided by Riedel-de Haën. Aqueous ammonium solution of 25 wt% was produced by VWR International Ltd. which was used to set the pH in catalyst preparation. During the CCVD syntheses nitrogen gas was used as both leacher and carrier gas and acetylene gas was the carbon precursor. Both gases were purchased from Messer. For nitrogen doping, tripropylamine (TPA) from Sigma–Aldrich with a purity of 98.5% was linked into the gas stream and as the nitrogen incorporation blocking agent ferrocene was utilized (Sigma–Aldrich, 98%).

For the purification and functionalization of the nitrogen-doped MWCNTs deionized water (MilliQ, 18.2 MΩ cm) and aqueous nitric acid solution of 65 wt% were used (the solution was purchased from VWR International Ltd.).

Reaction center proteins were isolated from *Rhodobacter sphaeroides* R-26 purple bacteria. Detergent was used to solubilize cell membranes (LDAO, N,N-dimethyl-dodecylamine-N-oxide, Fluka) then the protein was purified by ammonium sulfate precipitation and anion-exchange chromatography afterwards (DEAE Sephacel, Sigma–Aldrich). N-hydroxy-succinimide (98%, abbreviated as NHS) and N-cyclohexyl-N'-(2-morpholinoethyl)-carbodiimide methyl-p-toluenesulfonate (95%, abbreviated as EDC) were purchased from Sigma–Aldrich and were used as cross-linkers.

2.2 Catalyst preparation

A catalyst containing 5 wt% Fe and 5 wt% Co was prepared by the impregnation method. Measured amounts of Fe(III)-acetylacetonate, Co(II)-acetylacetonate, and CaCO₃ were taken, mixed in a beaker with distilled water, and then ultrasonicated for 15 min so the solvation and temporary dispersion were complete. Ammonia was added to the system to set and maintain a basic pH at around 9 and the dispersion was

heated to 90 °C and stirred until most of the water had evaporated. After the evaporation the catalyst was totally desiccated at 120 °C for 2 h.

2.3 Experimental system and syntheses

In this study, the CCVD method was utilized to synthesize nitrogen-doped MWCNTs. Nitrogen gas was passed through the reactor to maintain an inert atmosphere that prevents MWCNTs from oxidizing at higher temperatures but it did not take part in the nitrogen doping itself. Acetylene gas was introduced to the system as carbon precursor and TPA-supported carbon and nitrogen sources as well. Nitrogen and acetylene gases were mixed by passing through a Y-shaped tap. The liquid-phase TPA was joined in the system by two different methods, first by a bubbling technique, where the gases were conducted into liquid TPA, before the reactor, and the gas bubbles carried a convenient amount of TPA to the reaction site. In other cases, the TPA was led from a syringe pump through a special plug onto a steep quartz plate drop by drop that was located in a more heated area of the reactor. At higher temperature the liquid phase vaporized, thus at the reaction site it was already in gas phase.

In every experiment, 150 mg of the catalyst was measured and put into the quartz reactor. After 15 min of leaching, the reactor with nitrogen with a flow rate of 150 L h⁻¹ it was placed into the oven heated up to 720 °C. After the reactor was heated, the acetylene gas flow was set to 35 L h⁻¹ and the reaction process started. After the defined reaction time, the acetylene flow rate was set to zero and after 15 min of leaching the reactor was cooled to room temperature and the sample was collected.

As control samples nitrogen-doped MWCNTs were synthesized by both doping methods in syntheses where TPA was fed into the reactor during the whole reaction time. These experiments were carried out to get a wider range of nanostructures that help in the morphological evaluations. The reason why these nanoparticles were chosen to be the basis of comparison is because they most likely present nearly every possible type of deformation caused by nitrogen incorporation. The reaction times were 10, 20, and 30 min and the additional precursor stream—TPA—was introduced from the beginning of the syntheses. In the case of TPA injection, 5 mL of TPA was injected in every synthesis thus the effect of injection speed could also be examined later. During bubbling syntheses the TPA flow cannot be set and it highly depends on the environmental conditions as well.

In the following syntheses, TPA was conducted into the reactor after a certain time period and it was constant until the end of the syntheses. Then the total reaction time was 20 or 30 min the TPA stream was set for the last 5 and 10 min. Since the exact time required for the catalyst activation was not known, in the synthesis with 10 min reaction time the TPA streaming was reduced for only the last 2 min.

As ferrocene was proven to block nitrogen incorporation in carbon nanotube doping [25] the syntheses with

time-controlled injection were repeated once again with a mixture of 95 wt% TPA and 5 wt% of ferrocene.

2.4 MWCNT functionalization It is advisable for MWCNTs to be carboxyl functionalized in aqueous nitric acid solution with a concentration of at least 10 wt% for 1 h to achieve a proper level of functionalization. The main idea was that the nitric acid mainly targets those sites of MWCNTs where defects are located. To carry out functionalization the measured quantity of MWCNTs was dispersed in aqueous nitric acid solution of 5 and 10 wt% and this dispersion was stirred by a magnetic stirrer at room temperature for 15 and 30 min. After functionalization, the samples were washed with distilled water and put in a drier at 90 °C for 2 h.

2.5 Protein linking Carboxyl functionalized MWCNTs were dialyzed in phosphate buffer (pH = 7) for 17 h then it was ultrasonicated for 15 min. EDC was added to the dispersion to facilitate protein linkage and NHS was used for blocking the hydrolysis of the MWCNT–protein connection. After 2 h of dialysis, in order to remove the excess amount of cross-linking agents, purified RC-26 protein was mixed with the MWCNTs and the whole dispersion was stirred overnight at 4 °C then centrifuged and washed with the phosphate buffer solution. This process was repeated until the supernatant did not show traces of RC-26 during UV-vis examinations. The samples then had to be held in a freezer at a maximum temperature of –20 °C to prevent degradation (Fig. 1).

3 Results and discussion

3.1 Transmission electron microscopy studies In every case, the characterization started with TEM imaging (FEI, Technai G2 20 X-TWIN) as morphology and particle size play an important role in this study. First, the samples from control syntheses were examined. A small amount of each sample was dispersed in ethanol by ultrasonication then one or two small drops of this dispersion were placed on a 200 mesh Cu TEM grid with a carbon layer.

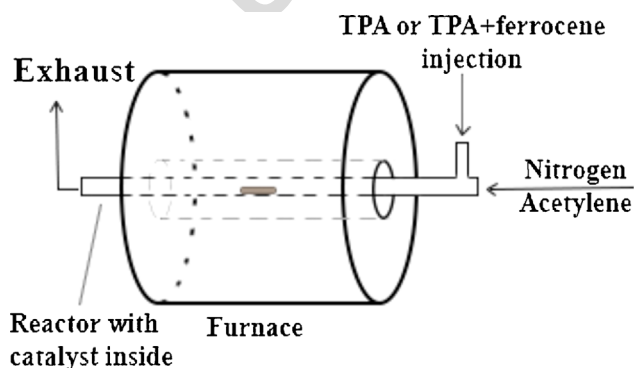


Figure 1 A schematic picture of the system applied for the syntheses.

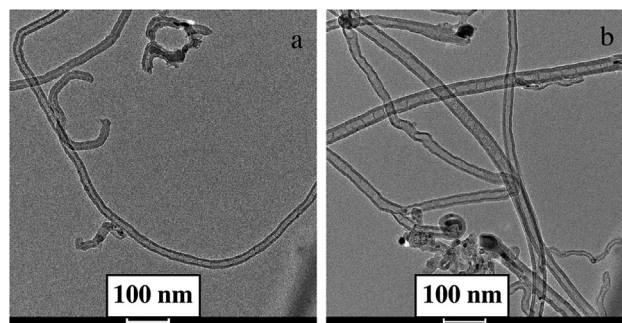


Figure 2 TEM images of control samples synthesized for 10 min (a) and 20 min (b).

The control samples were diverse but mainly both holey and bamboo-like MWCNTs could be seen (Fig. 2). Systematic deformation in the carbon nanotubes could not be observed.

In partial nitrogen doping, the best results were presented by those syntheses where the total reaction time was 20 min and the length of the injection period was 10 min. The expansion of the walls, Y-junctions, or other kinds of deformation could be observed at the end of the as-synthesized MWCNTs (Fig. 3b). Figure 4 shows a magnified area of Fig. 3b, where a MWCNT is observable with a structure close to holey MWCNTs in the middle segment but bamboo-like at both ends (marked with arrows). As this MWCNT encapsulates catalyst particles at both ends, it most likely had been synthesized in between the two active catalyst particles, and therefore the effects of partial nitrogen doping appear in the two closing segments of the MWCNT. In those cases where the total reaction time was 10 min, systematic changes cannot be observed and the deformations appear in a whole MWCNT or they do not appear at all. The reason for this is that the catalyst most probably activates around the end of the 10-min reaction time interval thus the TPA injection affects the whole synthesis process (Fig. 3a).

To make sure that these “anomalies” are caused by the nitrogen incorporation it had to be blocked and new samples

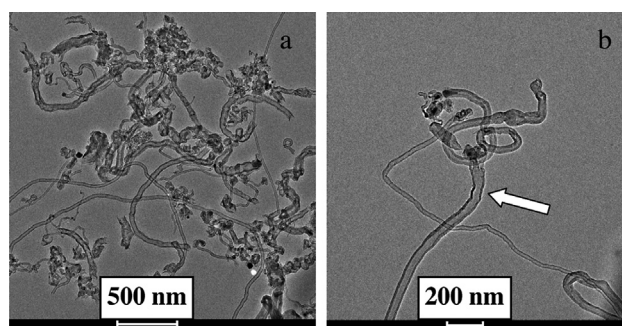


Figure 3 TEM images of synthesis samples from 10 min (with 2 min TPA injection) (a) and 20 min (with 5 min TPA injection) (b) reactions.

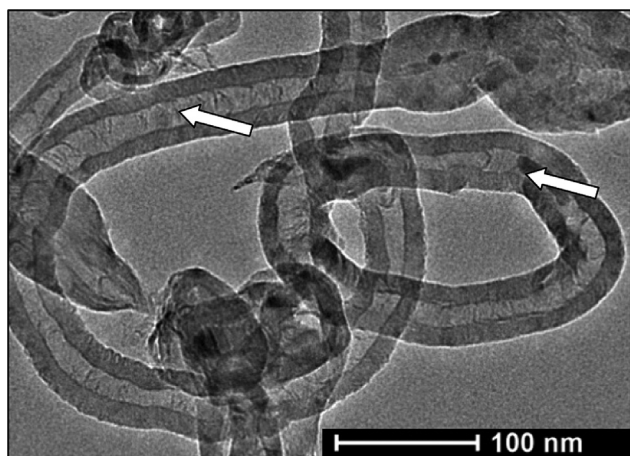


Figure 4 A magnified area of Fig. 3b.

had to be synthesized with the same reaction conditions as earlier. The results were as expected, blocking the nitrogen incorporation decreased the deformation at the end of the carbon nanotubes but they are similar to the samples synthesized with pure TPA injection (Fig. 5).

3.2 X-Ray photoelectron spectroscopy In order to be able to compare the samples and the effect of TPA injection time, modulation XPS studies of all samples were required. XP spectra were taken by a SPECS instrument equipped with a PHOIBOS 150 MCD 9 hemispherical analyzer. There was a certain deviation of data, but after recording several spectra from different areas of the samples it never exceeded 0.5%. Several samples of control syntheses were examined and the nitrogen content was mainly between 2–3%. The nitrogen content of samples synthesized with different intervals of TPA or TPA–ferrocene mixture injections is shown in Table 1. The binding energies corresponding to the pyridinic, pyrrolic, and other kinds of nitrogen incorporations are 398.5, 400.8, and 403.0 eV, respectively (Table 2).

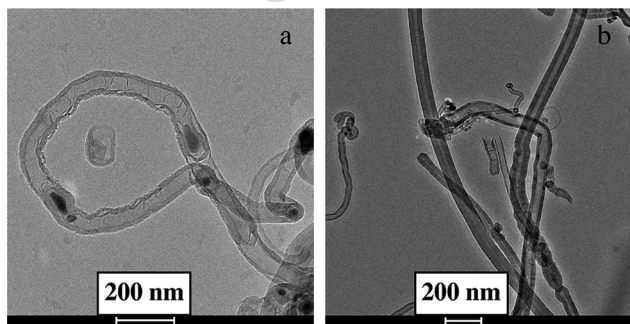


Figure 5 TEM images of samples synthesized for 20 min (with 10 TPA–ferrocene mixture injection) (a) and 30 min (with 5 min TPA–ferrocene mixture injection) (b).

Table 1 Nitrogen content of samples (sample name:total reaction time/TPA-injection time).

sample	nitrogen content	
	TPA injection (%)	TPA–ferrocene injection (%)
10/2	2.6	2.9
20/5	2.6	1.3
20/10	2.7	1.5
30/5	1.3	0.0
30/10	0.9	0.0

In the samples synthesized with TPA injection, an interesting case can be observed: nitrogen-doped MWCNTs synthesized for the same reaction time have a nitrogen content altering in the error interval, but after comparing all data it has to be said that a connection with the injection time cannot be stated, only relying on the XPS studies. The atomic ratios of nitrogen in the samples are around the 2–3% interval and they only differ for samples synthesized for 30 min. The reason of this phenomenon is that after a certain time period the inactivation of catalyst particles occurs and only a smaller amount of catalyst can help in the incorporation process of nitrogen atoms. The MWCNTs synthesized for 10 min have a structure diversity that does not fit our purposes, thus the best results, which have a more profound analysis later in this study, were shown by the samples synthesized for a total reaction time of 20 min and with 10 min of TPA injection.

When a mixture of 95 wt% TPA and 5 wt% ferrocene was injected into the reactor the nitrogen content of sample 10/2 did not change much. Taking the XP spectra of the other samples (20/5, 20/10, 30/5, and 30/10) a decreasing tendency of nitrogen content could be observed. The amount of nitrogen in samples synthesized for 20 min decreased with about 50%, thus the nitrogen incorporation blocking properties of ferrocene are confirmed by these measurements. The theory behind the fact that the nitrogen content did not change much in sample 10/2 is that ferrocene needs a certain time period for activation. In samples with a 30 min reaction time, the nitrogen content was 0.0%, which

Table 2 Nitrogen-content distribution in samples by TPA injection with/without ferrocene (sample name:total reaction time/TPA injection time).

sample	nitrogen content distribution (at%)		
	pyridinic	pyrrolic	other
10/2	47/46	40/40	13/14
20/5	52/37	37/40	11/23
20/10	43/49	44/51	13/0.0
30/5	46/–	51/–	4/–
30/10	44/–	40/–	16/–

can be the result of both the blocking of nitrogen incorporation and catalyst inactivation.

3.3 Diameter distribution On analyzing the TEM pictures the outer diameter distribution was obtained (Table 3). Both the diameters and the wall thickness increased with the reaction time, and in the case of delayed injection syntheses it was also dependent of the injection time itself. As expected, the smallest outer diameters were observed in samples where the nitrogen doping was blocked by ferrocene injection. The biggest outer diameters were obtained by partial doping syntheses. This is due to the effects of nitrogen shock that means that above a certain nitrogen flux in the reaction space the synthesis of well-structured material is less favorable because the decomposition of the precursors is faster than the synthesis of MWCNTs. In a lot of cases—as can be seen in Fig. 5b—it causes the disintegration of MWCNT walls which results in wall thickening and therefore an increase in outer diameter as well.

As mentioned earlier, the flow rate of the liquid precursors was chosen so as to inject 5 mL of them in the injection period. That is why the effect of nitrogen shock does not appear in control syntheses because the injection is slow, thus the nitrogen flux is lower. It is less likely observable in syntheses with the shortest injection times as well, because a certain time is needed for the nitrogen to affect the structure. MWCNTs with the biggest outer diameter were synthesized in the syntheses with 30 min reaction time because a significant number of the catalyst particles were inactivated and the decomposed material is less graphitic.

3.4 X-ray diffractometry XRD data were analyzed by a Rigaku Miniflex II diffractometer in order to determine if the samples possess graphitic structure. The evaluated measurements show the characteristic reflections of graphitic layers at around 26–26.5° and 44.5–45°. Comparing these results with TEM imaging, the nanotubular structure of samples is confirmed (Fig. 6). All the other reflections are

Table 3 Diameter distributions by TEM evaluation and their standard deviations (SD). Sample name: control samples or injected material total reaction time/injection time.

sample name	diameter (nm)	SD (nm)
Control 10	16	8
Control 20	22	7
Control 30	47	29
Ferrocene-TPA 10/2	11	4
Ferrocene-TPA 20/5	17	7
Ferrocene-TPA 20/10	21	10
Ferrocene-TPA 30/10	25	13
TPA 10/2	28	20
TPA 20/5	23	6
TPA 20/10	25	7
TPA 30/5	46	38
TPA 30/10	48	24

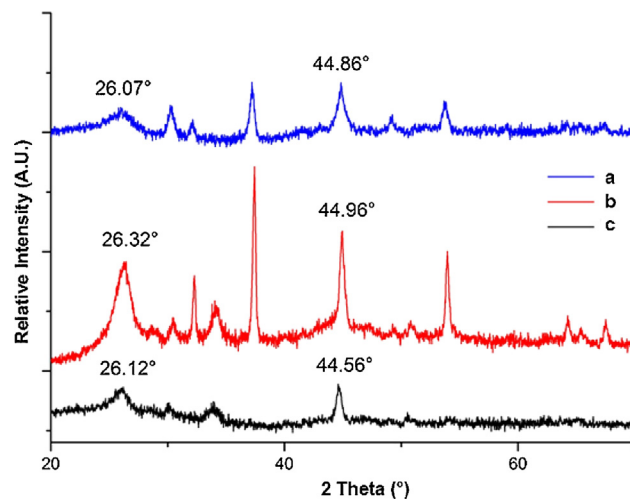


Figure 6 XRD diffractograms of control sample synthesized for 20 min (a) and 20/10 samples with TPA (b) and TPA–ferrocene injection (c)

from derivative compounds after heat treatment of Co, Fe, and Ca salts, as pristine samples after the syntheses were examined, catalyst particles could generate signals as well.

3.5 Raman spectroscopic examinations Raman measurements were carried out by a DXR Raman microscope operating with a 532 nm laser (Thermo Scientific). As incorporated nitrogen atoms can only support the MWCNT matrix with three bonding electrons, doping syntheses result in MWCNTs with more defect sites and also with a lower level of graphitization [17, 26]. Relying on this fact Raman spectra were evaluated to investigate the increase of defects caused by nitrogen incorporation. To find the connection between doping and the increment of the present of nongraphitic areas the spectra of samples with unblocked and blocked nitrogen incorporation had to be evaluated. Analyzing the D/G ratio of the two spectra (defect peak intensity/graphitization peak intensity) the effect of nitrogen bonding into the MWCNT matrix can be easily characterized. When pure TPA was injected into the reactor the D/G ratio was 1.28 (Fig. 7a), while the D/G ratio of the sample synthesized with TPA–ferrocene mixture injection was 0.97 (Fig. 7b). However, there are several peaks in the 2000–3000 cm^{-1} they cannot be declared to be overtones as there are other peaks (e.g., around 700 cm^{-1}) which are most probably noise. The D/G ratio is only counted from this spectrum for representative purposes, but it is overall true that all the spectra from samples prepared with TPA had a more intensive D peak than the G peak, and for samples synthesized with the injection of the mixture of TPA and ferrocene the G peak was always representing bigger values.

From this data, we can conclude that in those syntheses where nitrogen doping was blocked by ferrocene solution injection the level of graphitization was higher than in THE case of pure TPA injection. On analyzing the G-bands a downshift from 1583 to 1579 cm^{-1} is observable in the

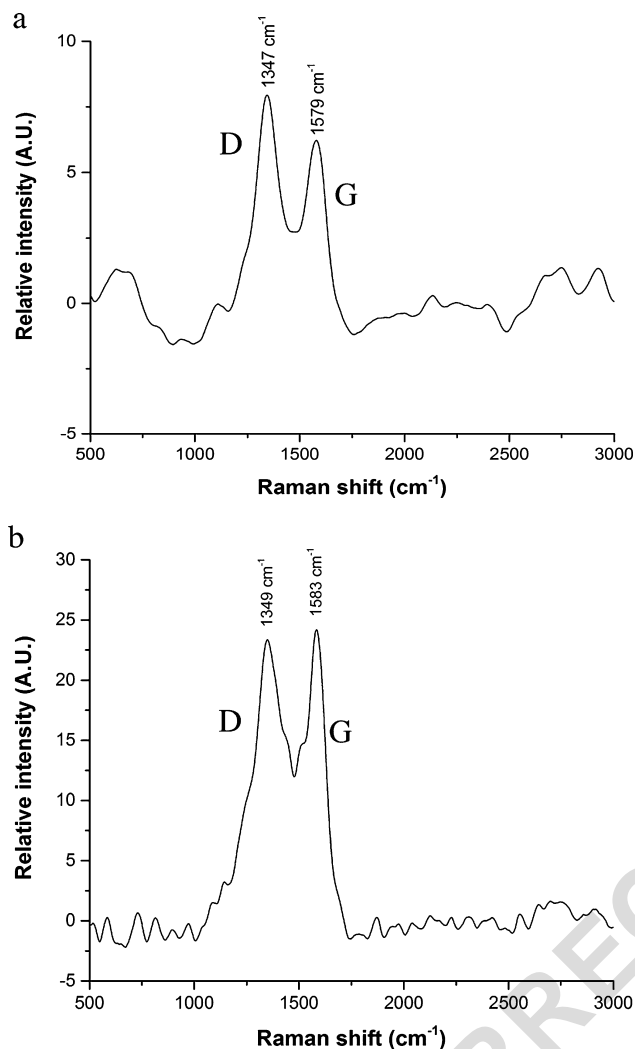


Figure 7 Raman spectrum of 20/10 samples synthesized with TPA (a) and TPA-ferrocene mixture injection (b).

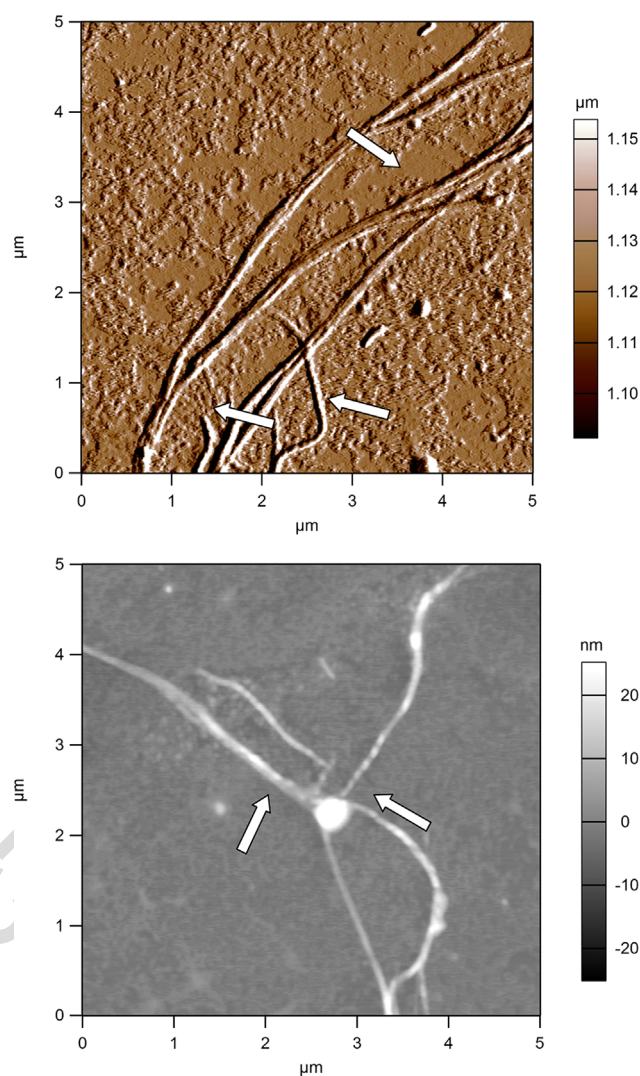


Figure 8 Amplitude (a) and height (b) AFM images of the protein-linked samples. Arrows point at possibly protein-linked segments.

spectrum of the nitrogen-doped sample. This might be the result of a charge transfer from the nitrogen atoms to carbon atoms, but the resolution of the spectra is comparable with the shifting thus clear conclusion cannot be stated. This phenomenon also appears in the case of D-bands, but the difference in wavelength is too small to consider.

3.6 Atomic force microscopy studies AFM measurements were carried out by an Asylum MFP-3D head and controller (Asylum Research, Santa Barbara, CA, USA) in tapping/noncontact (AC) mode. In the amplitude images (Fig. 8a), visible relative deviation from the surface can mainly be observed at the starting or ending section of the carbon nanotubes that confirms that the partial nitrogen doping and therefore the functionalization under light circumstances were successful in the way it was expected.

This derives from the synthesis method, as defects from nitrogen incorporation allow the functionalization under light

circumstances—after this process protein molecules can link to the functional groups—whereas pristine segments are less probably functionalized. The height images show that the deviation from the surface is around 10 nm that equals the diameter of the RC protein [16–18] (Fig. 8b).

4 Conclusions In this study, a new method was utilized to control the incorporation site of nitrogen during carbon nanotube doping. After the synthesis and purification processes, the functionalizing reactions were carried out in order to facilitate protein linkage. This step was necessary to enhance the observation's efficiency of the location of functional groups by electron microscopy. Several examination techniques helped in characterizing the samples. Our experiments indicated that syntheses, carried out in the new reactor, were successful and resulted in carbon nanotubes segmentally doped with nitrogen. TEM studies revealed that the expected deformations are localized only in a defined

segment of carbon nanotubes, therefore, nitrogen doping is most possibly presented there. The nitrogen content in the samples represented in atomic ratios was between 0.9% and 2.9%. The deformations facilitate the functionalization at that certain area thus the location of carboxyl groups can be determined. AFM studies after protein linking enforced the evidences of a successful series of experiments.

Acknowledgements The work was supported by the Swiss Contribution SH/7/2/20.

References

- [1] S. Iijima, *Nature* **354**, 56–58 (1991).
- [2] T. W. Odom, J.-L. Huang, and C. M. Lieber^{Q3}, et al., *Nature* **391**, 62–64 (1998).
- [3] J.-P. Salvetat, J.-M. Bonard, and N. B. Thomson, et al., *Appl. Phys. A* **69**, 255–260 (1999).
- [4] R. H. Baughman, A. A. Zakhidov, and W. A. de Heer, *Science* **297**, 787–792 (2002).
- [5] M. Paradise and T. Goswami, *Mater. Des.* **28**, 1477–1489 (2007).
- [6] M. Magyar, K. Hajdu, and T. Szabo, et al., *Phys. Status Solidi B* **250**, 2559–2563 (2013).
- [7] L. Lacerda, A. Bianco, and M. Prato, et al., *Adv. Drug Deliv. Rev.* **58**, 1460–1470 (2006).
- [8] X. X. XX^{Q4}, XXXX.
- [9] K. A. Wepasnick, B. A. Smith, and J. L. Bitter, et al., *Anal. Bioanal. Chem.* **396**, 1003–1014 (2010).
- [10] K. A. Wepasnick, B. A. Smith, and K. E. Schrote, et al., *Carbon* **49**, 24–36 (2011).
- [11] K. Nemeth, B. Reti, and K. Hernadi, et al., *Phys. Status Solidi B* **249**, 2333–2336 (2002).
- [12] N. Bendiab, A. Righi, and E. Anglaret, et al., *Chem. Phys. Lett.* **339**, 305–310 (2001).
- [13] K. C. Mondal, N. J. Coville, and M. J. Witcomb, et al., *Chem. Phys. Lett.* **437**, 87–91 (2007).
- [14] M. Glerup, M. Castignolles, and M. Holzinger, et al., *Chem. Commun.* **20**, 2542–2543 (2003).
- [15] Y. Zhang, J. Zhang, and D. S. Su, *ChemSusChem* **7**, 1240–1250 (2014).
- [16] D. Fejes and K. Hernadi, *Materials* **3**, 2618–2642 (2010).
- [17] G. C. Marjanovic, I. Pasti, and S. Mentus, *Prog. Mater. Sci.* **69**, 61–182 (2015).
- [18] P. Ayala, R. Arenal, and T. Pichler, et al., *Carbon* **48**, 575–586 (2010).
- [19] O. Y. Podyachevaa, and Z. R. Ismagilov, *Catal. Today* **249**, 12–22 (2015).
- [20] C. P. Ewels and M. Glerup, *J. Nanosci. Nanotechnol.* **5**, 1–19 (2005).
- [21] A. L. Mihalchik, W. Ding, and Y. Quian, et al., *Toxicology* **333**, 25–36 (2015).
- [22] M. Dorogi, Z. Balint, and L. Nagy, et al., *J. Phys. Chem. B* **110**, 21473–21479 (2006).
- [23] K. Hajdu, T. Szabo, and L. Nagy, et al., *Phys. Status Solidi B* **248**, 2700–2703 (2011).
- [24] H. Ohmori, L. Nagy, and M. Dorogi, et al., *J. Biophys. Lett.* **37**, 1167–1174 (2008).
- [25] R. M. Yadav, D. P. Singh, and O. N. Srivastava, et al., *J. Nanosci. Nanotechnol.* **5**, 820–824 (2005).
- [26] S. H. Lim, H. I. Elim, and J. Lin, et al., *Phys. Rev. B* **73**, 045402 (2006).

Q1: Author: Please confirm that given names (red) and surnames/family names (green) have been identified correctly.

Q2: Author: Figure 1 has not been mentioned in the text. Please cite the figure in the relevant place in the text.

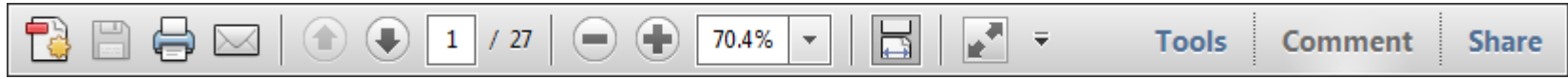
Q3: Author: For every reference in this reference list that has et al., please supply the names of all authors instead of using et al.

Q4: Author: Please provide Ref. [8].

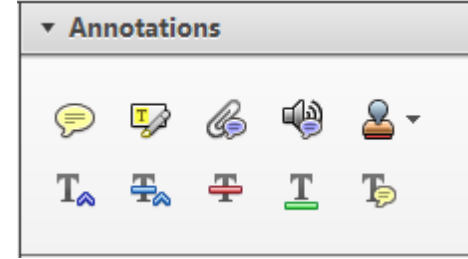
Required software to e-annotate PDFs: Adobe Acrobat Professional or Adobe Reader (version 8.0 or above). (Note that this document uses screenshots from Adobe Reader X)

The latest version of Acrobat Reader can be downloaded for free at: <http://get.adobe.com/reader/>

Once you have Acrobat Reader open on your computer, click on the [Comment](#) tab at the right of the toolbar:



This will open up a panel down the right side of the document. The majority of tools you will use for annotating your proof will be in the [Annotations](#) section, pictured opposite. We've picked out some of these tools below:



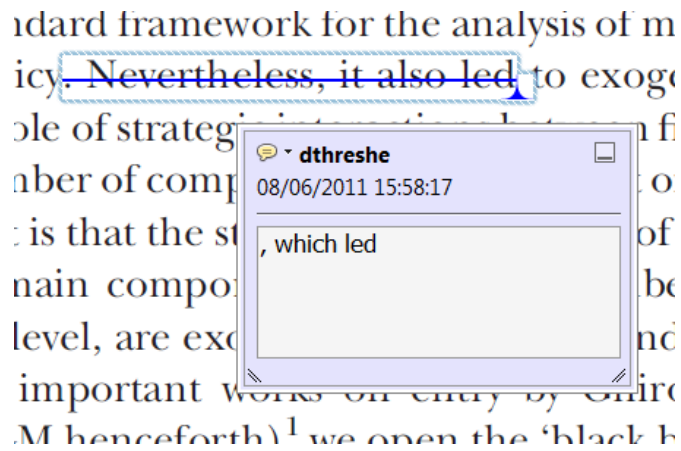
1. Replace (Ins) Tool – for replacing text.



Strikes a line through text and opens up a text box where replacement text can be entered.

How to use it

- Highlight a word or sentence.
- Click on the [Replace \(Ins\)](#) icon in the Annotations section.
- Type the replacement text into the blue box that appears.



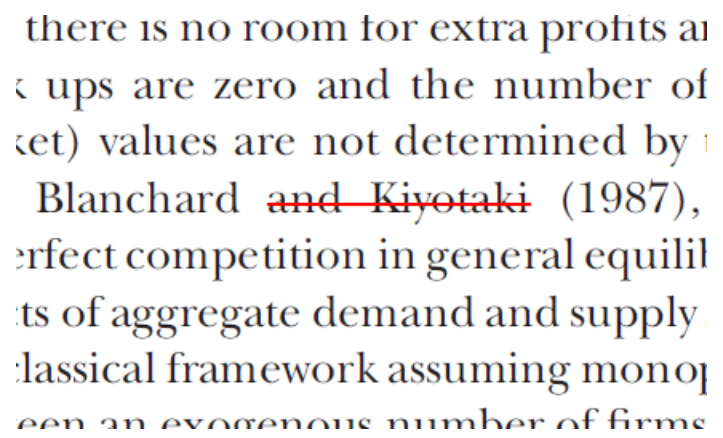
2. Strikethrough (Del) Tool – for deleting text.



Strikes a red line through text that is to be deleted.

How to use it

- Highlight a word or sentence.
- Click on the [Strikethrough \(Del\)](#) icon in the Annotations section.



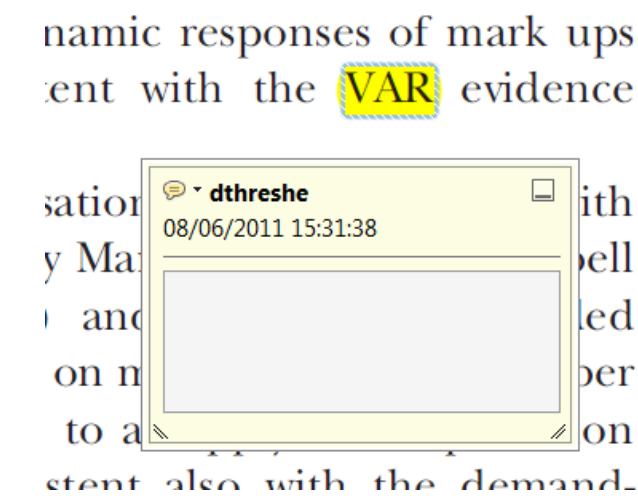
3. Add note to text Tool – for highlighting a section to be changed to bold or italic.



Highlights text in yellow and opens up a text box where comments can be entered.

How to use it

- Highlight the relevant section of text.
- Click on the [Add note to text](#) icon in the Annotations section.
- Type instruction on what should be changed regarding the text into the yellow box that appears.



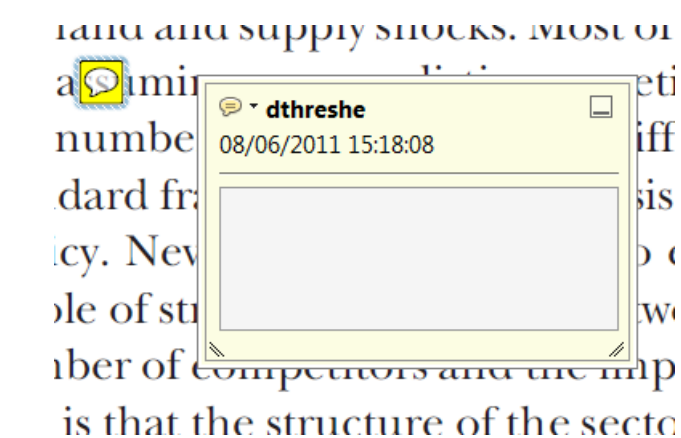
4. Add sticky note Tool – for making notes at specific points in the text.



Marks a point in the proof where a comment needs to be highlighted.

How to use it

- Click on the [Add sticky note](#) icon in the Annotations section.
- Click at the point in the proof where the comment should be inserted.
- Type the comment into the yellow box that appears.



USING e-ANNOTATION TOOLS FOR ELECTRONIC PROOF CORRECTION

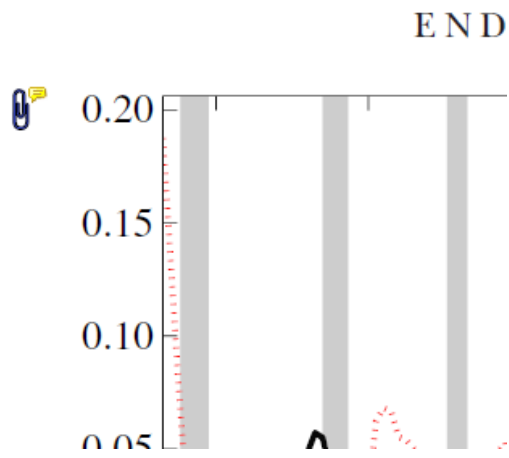
5. Attach File Tool – for inserting large amounts of text or replacement figures.



Inserts an icon linking to the attached file in the appropriate place in the text.

How to use it

- Click on the [Attach File](#) icon in the Annotations section.
- Click on the proof to where you'd like the attached file to be linked.
- Select the file to be attached from your computer or network.
- Select the colour and type of icon that will appear in the proof. Click OK.



6. Add stamp Tool – for approving a proof if no corrections are required.



Inserts a selected stamp onto an appropriate place in the proof.

How to use it

- Click on the [Add stamp](#) icon in the Annotations section.
- Select the stamp you want to use. (The [Approved](#) stamp is usually available directly in the menu that appears).
- Click on the proof where you'd like the stamp to appear. (Where a proof is to be approved as it is, this would normally be on the first page).

of the business cycle, starting with the
 on perfect competition, constant ret
 production. In this environment goods
 extra profits and the market for marke
 he market for goods is determined by the model. The New-Key
 otaki (1987), has introduced produc
 general equilibrium models with nomin
 and market-clearing. Most of this literat

APPROVED

Drawing Markups

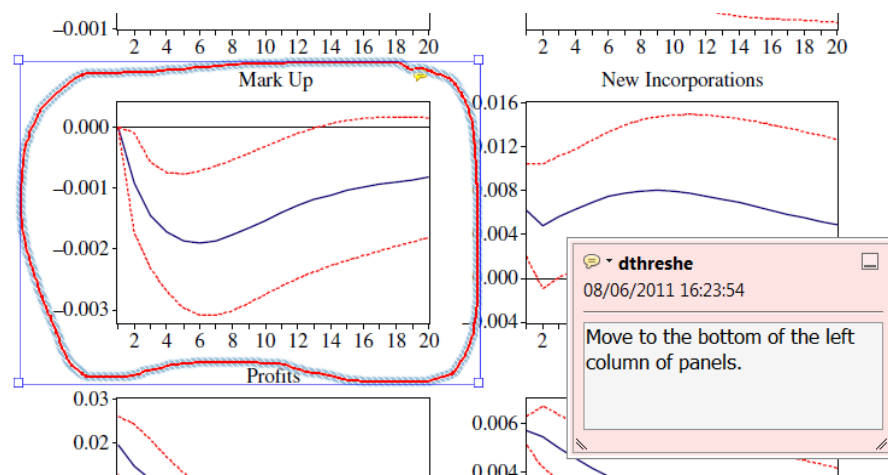


7. Drawing Markups Tools – for drawing shapes, lines and freeform annotations on proofs and commenting on these marks.

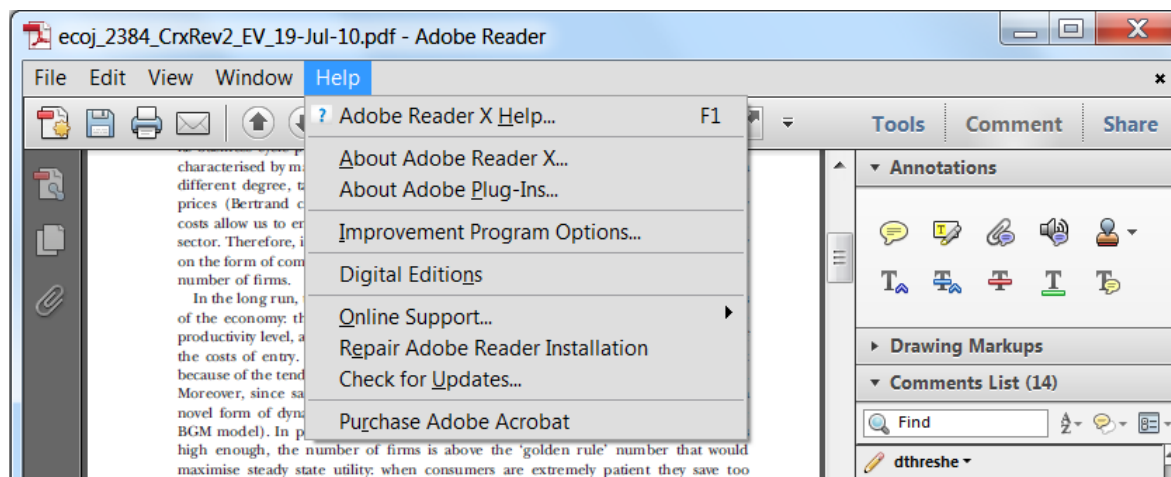
Allows shapes, lines and freeform annotations to be drawn on proofs and for comment to be made on these marks..

How to use it

- Click on one of the shapes in the [Drawing Markups](#) section.
- Click on the proof at the relevant point and draw the selected shape with the cursor.
- To add a comment to the drawn shape, move the cursor over the shape until an arrowhead appears.
- Double click on the shape and type any text in the red box that appears.



For further information on how to annotate proofs, click on the [Help](#) menu to reveal a list of further options:



Price List – pss (b) 201)

WILEY-VCH

Reprints/Issues/PDF-Files/Posters

The prices listed below are valid only for orders received in the course of 2015. Minimum order for reprints is 50 copies. **Reprints can be ordered before and after publication of an article. All reprints are delivered with color cover and color figures.** If more than 500 copies are ordered, special prices are available upon request.

Single issues are available to authors at a reduced price.

The prices include mailing and handling charges. All prices are subject to local VAT/sales tax.

Reprints with color cover Size (pages)	Price for orders of (in Euro)					
	50 copies	100 copies	150 copies	200 copies	300 copies	500 copies*
1–4	345	395	425	445	548	752
5–8	490	573	608	636	784	1077
9–12	640	739	786	824	1016	1396
13–16	780	900	958	1004	1237	1701
17–20	930	1070	1138	1196	1489	2022
for every additional 4 pages	147	169	175	188	231	315
for personalized color cover	190	340	440	650	840	990

PDF file (300 dpi, unlimited number of printouts, customized cover sheet) € 330

Issues € 36 per copy for up to 10 copies.*

Cover Posters

- A2 (42 × 60 cm/17 × 24in) € 49
- A1 (60 × 84 cm/24 × 33in) € 69

*Prices for more copies available on request.

Special offer: If you order 100 or more reprints you will receive a pdf file (300 dpi, unlimited number of printouts, color figures) and an issue for free.

Color figures

If your paper contains **color figures**, please notice that, generally, these figures will appear in color in the online PDF version and all reprints of your article at no cost. The print version of the figures in the journal hardcopy will be black/white unless the author explicitly requests a color print publication and contributes to the additional printing costs.

Approximate color print figure charges

First figure	€ 495
Each additional figure	€ 395 Special prices for more color print figures on request

If you wish color figures in print, please answer the **color print authorization** questions on the order form.